The magnetic field created by this antenna was measured at the distance 1200 km from the transmitter, in the Barentsburg Observatory, by a three-component induction magnetometer. The radiation experiments were conducted within a few days, mostly at night, when the IAR formation probability is high.

The main result of these experiments is that in a number of cases, a nonmonotonic dependence of the received signal on the frequency was detected for the horizontal magnetic field component (Fig. 5b, c). We believe that this is due to the IAR influence on the propagating signal, because the scheme of the experiment allowed investigating the field in the region with a significant contribution of the wave propagating in the outer waveguide (above the F-layer) to the total field.

We also estimated the effectiveness of various ionospheric models for interpretation of the results of the conducted measurements. We showed that the results of the international reference ionosphere (IRI) model calculations agree poorly with the experimental data. The upper atmosphere model (UAM) calculations better correspond to the experiment, but they are also imperfect. The results of experimental ionospheric studies (such as satellite tomography) should be used to refine the ionospheric characteristics obtained by model calculations.

5. The future of geophysical investigations in Spitsbergen

The future of geophysical investigations in Spitsbergen is seen, first, in increasing international cooperation. The times have passed when observations were made in isolation and only data from two or three instruments were used to analyze phenomena. Studies by Russian, Norwegian, Swedish, Finnish, and Chinese researchers clearly demonstrate the effectiveness of coordinated observations and a comprehensive approach to data analysis. Understanding that, in 2009 the Norwegian Research Council put forward an initiative to integrate the maximum possible number of observation points operating in Spitsbergen into a unified measurement–information system aimed at the global modeling of the Arctic atmosphere. This Svalbard Integrated Observing System (SIOS) project was financially supported by the European Union. The Polar Geophysical Institute is a member of the consortium running the preliminary stage of the project; it is part of a group researching the influence of magnetospheric processes on the Arctic climate.

References

1. Kunitsyn V E, Tereshchenko E D, Andreeva E S *Radiotomografiya Ionosfery* (Radiotomography of the Ionosphere) (Moscow: Fizmatlit, 2007)
2. Frolov V L et al. *Usp. Fiz. Nauk* **177** 330 (2007) [*Phys. Usp.* **50** 315 (2007)]
3. Sandholt P E et al. *J. Geophys. Res.* **103** (A10) 23325 (1998)
4. Vorobjev V G et al. *Planet. Space Sci.* **23** 269 (1975)
5. Kozlovsky A, Kangas J *J. Geophys. Res.* **107** (A2) 1017 (2002)
6. Kozlovsky A E et al. *Ann. Geophys.* **21** 2303 (2003)
7. Safargaleev V et al. *Ann. Geophys.* **26** 517 (2008)
8. Thidé B, Kopka H, Stubbe P *Phys. Rev. Lett.* **49** 1561 (1982)
9. Tereshchenko E D et al., in *VII Intern. Suzdal URSI Symp. "Modification of Ionosphere by Powerful Radio Waves," Book of Abstracts* (Moscow, 2007) p. 42
10. Tereshchenko E D et al. *Ann. Geophys.* **24** 1819 (2006)
11. Polyakov S V, Rappoport V O *Geomagn. Aeron.* **21** 610 (1981)

PACS numbers: **94.20.–y**, 94.50.Ci, **96.30.–t**
DOI: 10.3367/UFNe.0180.201005j.0542

Results of solar wind and planetary ionosphere research using radiophysical methods

N A Armand, Yu V Gulyaev, A L Gavrik, A I Efimov, S S Matyugov, A G Pavelyev, N A Savich, L N Samoznaev, V M Smirnov, O I Yakovlev

1. Introduction

We describe the results of space plasma studies using remote methods developed at the Kotelnikov Institute of Radioengineering and Electronics (IRE) of the Russian Academy of Sciences. The main result of circumsolar plasma research is the determination of the radial velocity dependence for the motion of plasma fluxes and solar wind turbulence modes at various distances from the Sun. Priority data on altitude profiles of Martian and Venusian night ionospheres have been obtained using the radio sensing method. Two monitoring methods for Earth's ionosphere have been suggested and realized. In the first method, ionospheric radio sensing is done on the spacecraft–Earth's surface point path. In the realization of the second method, two Earth satellites are used, one of which is the source of radio waves sounding the ionosphere, and the other is the receiver of plasma-modified signals.

The aim of this contribution is to briefly describe the main results of various space plasma studies done at the IRE, Department of Space Radiophysics, from 1970 to 2009. The work performed was devoted to investigations of solar wind and Martian and Venusian ionospheres, and to the development of new monitoring methods of Earth's ionosphere by using spacecraft signals. In Figure 1, dashed lines show the radio wave propagation paths from spacecraft to points on Earth's surface. For solar wind research, we used signals of Soviet (Mars-2 and Venera-10 (-15,-16)), European (Helios and Ulysses), and American (Galileo and MGS (Mars Global Surveyor)) spacecraft. It was possible to investigate the plasma shells of Mars and Venus after the Soviet Mars-2 and Venus-9 (-10) spacecraft were launched into the first artificial satellite orbits of these planets. The monitoring of Earth's ionosphere by a new radio sensing method was realized on satellite–satellite paths. For this, we have used radio links between the Mir Station and geostationary satellites, as well as between GPS (Global Positioning System) satellites and the research CHAMP (Challenging Minisatellite Payload) and FORMOSAT-3 satellites. At the first stage, the influence of various media on the amplitude, phase, frequency, and spectrum of decimeter radio waves was

N A Armand, Yu V Gulyaev, A L Gavrik, A I Efimov, S S Matyugov, A G Pavelyev, N A Savich, L N Samoznaev, V M Smirnov, O I Yakovlev
Kotelnikov Institute of Radioengineering and Electronics, Russian Academy of Sciences, Fryazino branch, Fryazino, Moscow region, Russian Federation
Email: efimov@ms.ire.rssi.ru

Uspekhi Fizicheskikh Nauk **180** (5) 542 – 548 (2010)
DOI: 10.3367/UFNr.0180.201005j.0542
Translated by S V Vladimirov; edited by A M Semikhatov

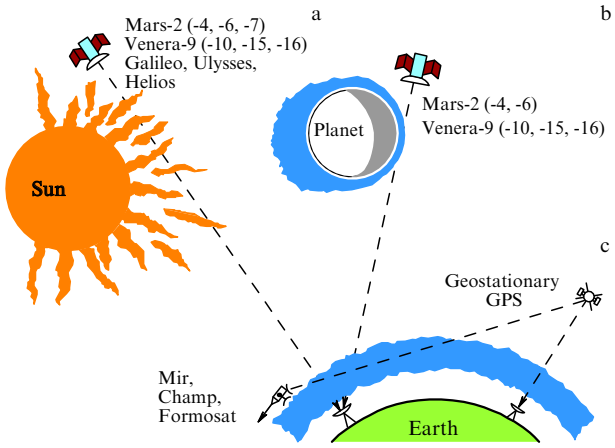

Figure 1. Scheme for radio sensing of circumsolar plasma (a), planetary ionospheres (b), and Earth's ionosphere (c).

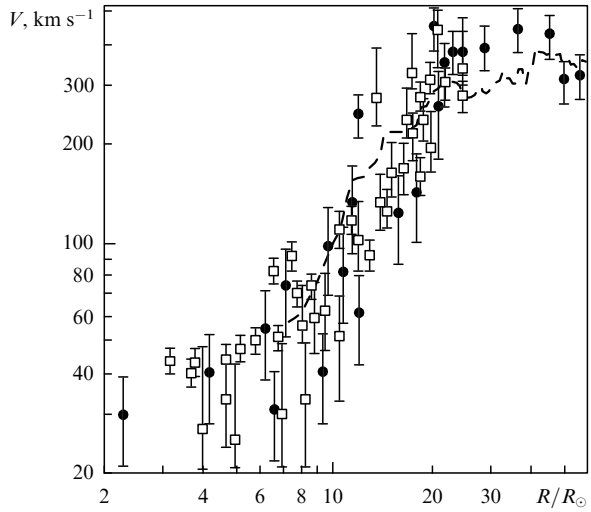

Figure 2. The solar wind velocity dependence on the heliocentric distance according to radio sounding data. Black dots correspond to Venera-10 data, 1976; squares, to Venera-15 (-16) data, 1984; the dashed line, to Galileo data, 1997.

studied. Results of this first stage are published in [1]. At the second stage, inverse problems were solved: the plasma parameters at various distances from the Sun or planetary surfaces were determined using radio data. This contribution describes the main results of the second stage of research.

2. Solar wind investigation

At the beginning of our studies, it had been known that solar wind plasma fluxes are strongly nonuniform and the speed of their motion near Earth is 300 – 400 km s^{-1}. The region of solar wind formation and acceleration, located at heliocentric distances in the range 2–40 solar radii R_0, was poorly investigated. In particular, the main theoretical difficulty was that the initial plasma energy near the Sun was insufficient for solar wind acceleration up to supersonic speeds.

First of all, it was necessary to obtain the experimental dependence of the solar wind velocity V on the heliocentric distance R, localize the transition from subsonic to supersonic flows of plasma streams, and find the region of sharp solar wind acceleration. We performed several long-term cycles of circumsolar and interplanetary plasma radio sounding using deep-space communication centers separated over large distances. Moving plasma inhomogeneities lead to correlated fluctuations of radio wave frequencies on diverse paths, which allows measuring the time delay of such fluctuations at one point compared to that at another point, and thus determining the solar wind velocity. Figure 2 shows the dependence of the solar wind velocity V on the heliocentric distance R in terms of the solar radius R_0, obtained in 1976 and 1984 by Venera-10 (-15, -16) spacecraft. The first experimental dependence $V(R)$ showed that the main plasma acceleration occurs over the distances $(8-20)R_0$. In the region $(7-12)R_0$, a transition from the subsonic to the supersonic state occurs, and at $R > 40R_0$, the velocity is stabilized at 300 – 400 km s^{-1}.

In 1996 – 1997, on the basis of Galileo spacecraft radio sensing data collected in collaboration with European researchers, the $V(R)$ dependence, shown in Fig. 2 by a dashed line, was also obtained. This result fully confirmed the accuracy of the above conclusions on the solar wind velocity regime in the region of its main acceleration.

It was proposed that the effect of rapid solar wind acceleration is due to intensive Alfvén waves arriving from the corona; these waves transfer additional energy to solar wind via dissipation. To confirm this hypothesis, the Alfvén waves needed to be detected in the corona and supercorona of the Sun. On the basis of the analysis of polarization angle variations (Faraday rotation) of linearly polarized radio waves sounding the plasma, and with the use of a correlation analysis procedure for the Faraday rotation fluctuations observed at points on Earth's surface separated by a long distance, it was established that intensive Alfvén waves indeed exist at distances $(4-10)R_0$ and move with velocities 400 – 1000 km s^{-1}.

Solar wind can be regarded as a statistically nonuniform medium, similar to a turbulent gas. In this approach, three characteristics are introduced into the theory: the index p of the power-law spatial spectrum of inhomogeneities, the minimum scale l, and the maximum external scale L_0. At small distances from the Sun ($R < 60\,R_0$), these characteristics can be determined by the radio sounding method only, by analyzing fluctuations of the radio wave phases, frequencies, and amplitudes. Figure 3 shows the experimental dependence of the spectral index p of the spatial inhomogeneity on the heliocentric distance. It follows from the presented data that for $R > 25\,R_0$, the medium is indeed similar to a turbulent gas, with $p \approx 3.7$ (this corresponds to the Kolmogorov spectrum), the index p monotonically decreases for $R < 18\,R_0$, and for distances $(4-6)R_0$, we have $p \approx 3$, which is characteristic of plasma waves. The black dots give the values of p obtained in the solar wind sounding by the Venera-15 (-16) spacecraft (1984). The low values of the spectral index in the region of small distances $R < 10\,R_0$ correspond to small-scale inhomogeneities. The dashed line in Fig. 3 characterizes the data obtained in 1997 experiments of solar wind radio sensing by signals from Jupiter's European satellite, Galileo; these experimental data were processed at the IRE and published in collaboration with the researchers who had performed the experiment.

The spatial spectrum of inhomogeneities is also described by two characteristic linear scales. The maximum scale L_0 is related to features of plasma emission from various regions of the solar low corona: it is proportional to the distance R. Near

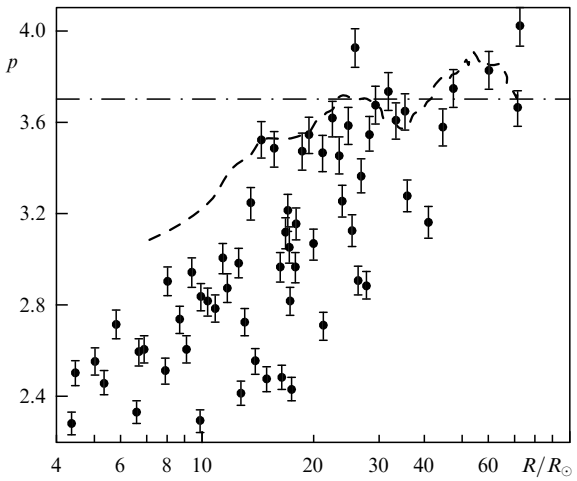

Figure 3. The spectral index of the spatial turbulence spectrum of solar plasma according to the radio sounding data by Venera-15 (-16) spacecraft, 1984 (black dots), and by Galileo spacecraft, 1997 (the dashed line).

the corona, the maximum scale is of the order of the Sun's radius. The minimum scale determines the characteristic sizes of the medium inhomogeneities at which energy is rapidly transferred from turbulence or wave phenomena into heat, i.e., plasma heating occurs. Apparently, the minimum scale l approximately corresponds to the proton gyroradius, and its value also increases with the distance from the Sun.

Thus, both characteristic scales in the solar wind inner regions increase approximately linearly with the increase in the heliocentric distance. The inertial interval width of the spectrum of plasma inhomogeneities, which occupies about four orders in magnitude, remains approximately the same at various distances from the Sun. However, processes responsible for the evolution of the index p for the external and internal scales are different.

The main results of solar wind investigations were obtained for the equatorial region of solar wind [2–12]. Recently, reliable data on solar wind emitted by high-latitude regions of the solar corona, where the plasma flow velocities are very large, were obtained by the radio sounding method.

3. Results of Martian and Venusian ionospheric studies

The investigation of ionospheres using the radio sounding method is possible when a spacecraft emitting radio signals immerges into or emerges from the planetary radio shadow, and the receiver on Earth records signals transformed by the planetary atmosphere. The radio sounding method uses a relation of the radio wave frequency and amplitude changes caused by the medium to the refraction angle, which is in turn related to the altitude profile of the ionosphere refractive index and hence to the electron concentration. To realize two-frequency radio sounding, centimeter- and decimeter-range transmitters ($\lambda_1 = 8$ cm and $\lambda_1 = 32$ cm) were installed on Mars-2 (-4) and Venera-9 (-10,-15,-16) spacecraft, and the reduced frequency difference and the amplitude variations of the mutually coherent signals were registered on Earth.

For the first time, a two-frequency radio sounding experiment was carried out to investigate the Martian ionosphere in 1971 when the Mars-2 spacecraft was covered by the planetary disk. The radio sounding was done on the sunlit side of the planet, the zenith angle Z_0 was 50° at the tangent point. As a result of data processing, the height distribution of the electron concentration $N(h)$ was obtained. The next experiment was conducted in 1974. In this case, the signals of the Mars-4 spacecraft sounded the evening-time ionosphere of Mars at $Z_O = 82°$. The concentration at the maximum was 5.9×10^4 cm^{-3} at the altitude 140 km, and the extent of the ionosphere was about 300 km high. When the Mars-4 spacecraft emerged from radio shadow, radio sounding of the dark side of Mars was done, by which the night-time ionosphere of this planet was detected for the first time. The ionization maximum appeared at the height 110 km, with the concentration $\approx 4.6 \times 10^3$ cm^{-3}, and the half-thickness of the main layer was about 35 km. Figure 4a shows the electron concentration profiles in the Martian ionosphere obtained by the radio sounding method for different conditions of solar illumination. On the daytime side, the ionosphere has the main maximum and lower maximum regions in which the concentration decreases with an increase in the zenith angle of the Sun. The plasma concentration and the height extent of the nighttime ionosphere are much less than those of the daytime one.

The experiments on multiple radio sounding of the Venusian ionosphere were conducted in October–December of 1975 using Venera-9 (-10) satellites. Data processing allowed determining 13 vertical profiles of the electron concentration in the daytime ionosphere and 22 distributions in the night-time one. The obtained results have a priority character, because data on the Venusian ionosphere had been quite scarce before these experiments with the Venus-9 (-10) satellites.

In 1983–1984, another major series of radio occultation experiments was conducted using the Venera-15 (-16) spacecraft: overall, 155 altitude profiles of the electron concentration $N(h)$ (73 profiles for the daytime ionosphere, 62 profiles for the night-time one, and 20 profiles for the terminator region) were obtained. The successful realization of multiple experiments allowed revealing the behavior patterns of the Venusian ionosphere under various illumination conditions. Figure 4b shows three distributions of the electron concentration characterizing the main properties of the daytime ionosphere of Venus. It was established that the concentration at the main ionization maximum naturally decreases with an increase in the solar zenith angle Z_O, from 5×10^5 cm^{-3} at $Z_O \approx 0$ to 2×10^4 cm^{-3} at $Z_O \approx 80° - 90°$. The height of the main maximum slightly depends on Z_O and is about 140 km. At the height 130–135 km, a regular presence of the lower ionization maximum was detected. A regular presence of the lower ionosphere at heights $h < 120$ km was discovered, with the additional maxima of the electron concentration. The distribution $N(h)$ in the upper ionosphere at heights $h > 200$ km is variable, the height of the upper ionosphere boundary tending to increase with increasing Z_O. At small Z_O (line *2*), it is about 270 km, and the upper boundary height increases (line *3*) with increasing Z_O.

Figure 4b also shows the electron concentration distributions in the night-time ionosphere of Venus that characterize its basic properties (curve *1*). The night-time ionosphere consists of one or two thin ionized layers of the half-thickness 5–10 km. The characteristic feature of the night-time ionosphere is its strong variability: the concen-

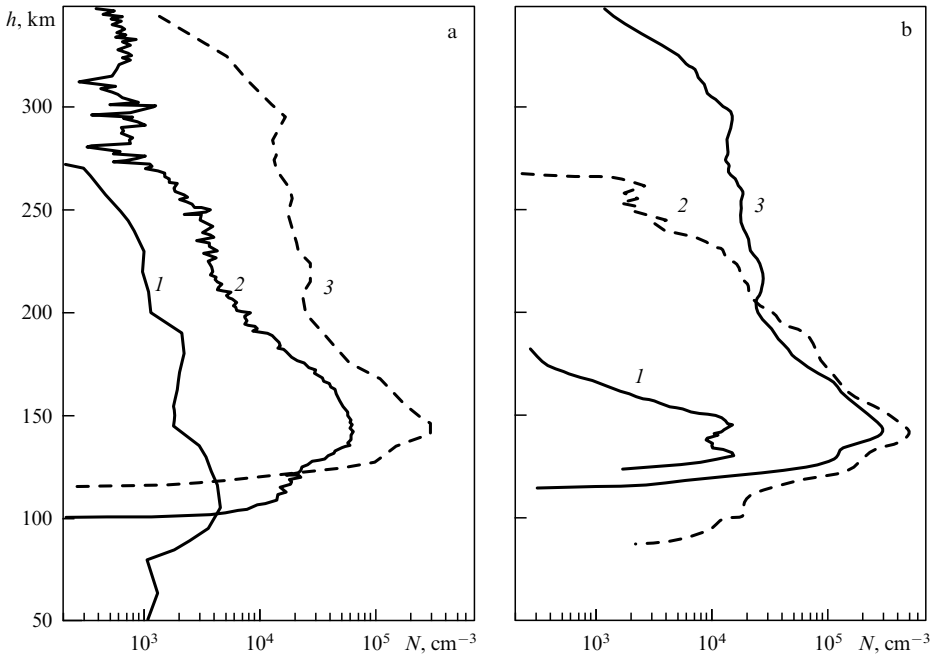

Figure 4. Examples of the electron concentration height distributions $N(h)$ in the Martian and Venusian ionospheres: (a) the distribution $N(h)$ for the night-time (*1*), evening time (*2*), and daytime (*3*) ionosphere of Mars; (b) the distribution $N(h)$ for the night-time ionosphere of Venus (*1*), for the ionosphere at a small zenith angle ($Z_O = 10°$) (*2*), and at a large zenith angle ($Z_O = 72°$) (*3*).

tration in the ionization maximum changes from 3×10^3 cm^{-3} to 2×10^4 cm^{-3}. The shape of the $N(h)$ profile also changes, as do its height extent, the half-thickness of the layers, and the heights of their maxima. The average height of the main ionization maximum is ≈ 140 km, and the values for the upper boundary height of the night-time ionosphere change in the range 140 – 250 km.

The electron concentration height profiles of the Martian and Venusian ionospheres obtained by the radio sounding method, as well as the local measurement data of the atmospheric gas composition, temperature, and ion composition in planetary neighborhoods, created a basis for the theory of ionosphere formation for Earth-group planets. Because the atmospheric gas composition for Mars and Venus is approximately identical, the ionospheric formation processes for these planets are also similar. The regions of the main and lower maximum in the daytime Martian and Venusian ionospheres are formed by photochemical processes, and molecular oxygen ions prevail there. In the upper ionosphere, the dominant role is played by the vertical diffusion of atomic oxygen ions and by the solar wind pressure. The night ionosphere of Venus is probably supported by two ionization sources: one of them is related to superthermal electron fluxes, and the other to the transport of atomic oxygen ions from the day side to the night side of the planet, with their subsequent diffusion downwards. The main results of the Martian and Venusian ionospheric research can be found in Refs [13 – 18].

The high accuracy of the two-frequency method allowed discovering the circumlunar plasma with the electron density 400 – 800 cm^{-3} by using the data of radio occultation experiments with the Luna-19 satellite [19], and discovering the plasma shell of Halley's comet with the electron density $10^3 - 3.6 \times 10^3$ cm^{-3} by using Vega-1 (-2) satellites [20, 21].

4. Development of methods to monitor Earth's ionosphere

We successfully developed two new methods for monitoring Earth's ionosphere. In the first method, the radio communication lines between GPS satellites and points on Earth's surface are used, and in the second one, radio sounding is carried out on a satellite–satellite path. The GPS and GLONASS (Global Navigating Satellite System) navigating systems provide a unique possibility to obtain data on the height distribution of the electron concentration in Earth's ionosphere via the radio translucence method with the use of navigating satellite–Earth point paths (the first method) for various helio- and geophysical conditions at any time in various regions on Earth. The measured parameters of radio signals (phase or delay time) contain information on the integrated characteristics of the medium through which the radio waves propagate. Determining the pseudorange difference, measured at two frequencies, is equivalent to determining the integrated electron concentration in the ionosphere. Variations of the measured ranges and distribution times (the phase or time delay) of radio signals are caused by variations of the radio wave refraction factors in space and time. This method is based on the dependence of the characteristics of received radio waves on the electron concentration distribution of the ionosphere. Mathematically, this dependence is described by a Fredholm integral equation of the first kind that has no analytic solution and requires elaboration of inversion methods for a class of ill-posed problems. The availability of high-speed computers allows using these methods for the inversion of observed data of radio signal parameters and for the prompt determination of the electron concentration height profile. The algorithm for the solution of such inverse problems, unstable by their nature, requires the use of special mathematical methods capable of incorpor-

ating additional information about the problem. Such information is given by models of the electron concentration distribution, for example, IRI (International Reference Ionosphere). Based on this model, we developed an effective solution method for the inverse problem of ionospheric radio translucence on a satellite–Earth path, using the relation between the parameters of sounding signals and the electron concentration height profile. This allowed developing the continuous monitoring technology intended to reconstruct the space and time structure of the ionosphere. The developed method can be used to recover the electron concentration height distribution of the ionosphere in the range of heights from 100 to 1000 km with the error ± 0.02 NU (1 NU $= 10^6$ electrons in 1 cm^3). The electron concentration value at the height of the ionosphere maximum is determined up to ± 0.014NU. The use of model assumptions about the ionosphere in the method developed by us leads to an essential decrease in the time needed to compute the determination of the electron concentration profile.

Figures 5a and 5b show examples of the obtained profiles $N(h)$ and, for comparison, the vertical sounding ionosonde data, together with computation results based on the IRI model. In using this method to determine the electron concentration in the ionosphere over a certain territory, it is possible to reveal the presence of peculiar features in the ionospheric plasma spatial distribution, because more than 10,000 altitude profiles of the electron density can be obtained for a site with a radius up to 1000 km from one Earth point within 24 hours. Examples of the profiles for one point are given in Fig. 5c. The radio translucence method allows finding the electron concentration distribution in the ionosphere in real time at any place on the globe by observations from a point located on Earth's surface, which is important for remote regions and those that are difficult to access [22–24]. This method can serve as an element in the global monitoring system of the Earth ionosphere.

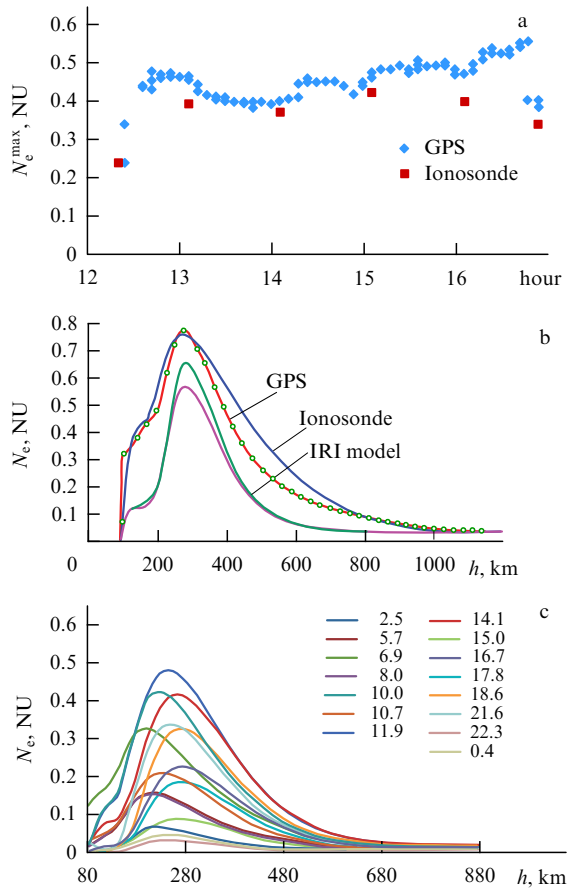

Figure 5. The electron concentration determined from GPS satellite observations, compared with ionosonde data.

For global ionosphere monitoring, a second method also turned out to be effective: radio occultation sounding using satellite–satellite paths. It was shown during the first radio occultation ionospheric experiments conducted on a path between the Mir orbital station and a geostationary satellite that this method gives detailed information on the electron concentration height profile in the lower ionosphere at heights 80–150 km. Signals from GPS satellites received by low-orbiting CHAMP and FORMOSAT-3 spacecraft were used for extensive radio sounding of the lower ionosphere across all regions on Earth at various solar illumination and activity. The ionosphere sounding data on satellite–satellite paths were processed in collaboration with researchers from the Geophysical Center in Germany and the Center for Space and Remote Sensing Research in Taiwan. Sporadic ionospheric formations at heights 85–120 km are especially clear in the radio data. Variations of the radio wave phase and amplitude accurately trace features of the electron concentration height profiles of E_s-structures, and it is therefore possible to determine the upper and lower boundaries of these structures with an error not exceeding ± 1 km. Detailed statistical data on the probability of the occurrence of E_s-structures in the equatorial, mid-latitude, and polar regions in daytime and night-time conditions were obtained. By this method, amplitude and phase radio wave fluctuations caused by small-scale plasma inhomogeneity in the F-layer were investigated. The intensity and spectrum of the inhomogeneities are changed under the action of solar wind shock waves. There is a stable connection between two events — the solar wind shock wave arrival on Earth and the occurrence of sporadic formations in the lower night-time polar ionosphere with an increased electron concentration and increased intensity of a small-scale plasma inhomogeneity in the F-layer. The radio sounding method on satellite–satellite paths allowed relating the following phenomena: the solar wind shock wave arrival $\Rightarrow$ proton and electron precipitation from the radiation belt $\Rightarrow$ excitation of a small-scale plasma inhomogeneity in the F-layer of the ionosphere $\Rightarrow$ appearance of intensive E_s-structures in the polar ionosphere. It is known that the occurrence of E_s-structures can be caused by different factors. The radio occultation sounding method confirmed the known fact that the probability of the occurrence of E_s-structures in the equatorial regions is independent of solar activity. According to our data, thin E_s-structures are often observed in these regions during both daytime and night-time, and their parameters do not change, even after the arrival of solar wind shock waves of the highest intensity.

Currently, due to the efforts of American, Taiwanese, and German researchers, an international system of radio occultation monitoring of the atmosphere and ionosphere is being formed that provides more than 2500 radio sounding sessions of Earth's atmosphere and ionosphere every day. At our institute, a radio occultation database has been created and is being continuously replenished. This requires elaboration of an automated processing of primary data methods. In the analysis of E_s-structures, the criterion for the appearance of intensive sporadic structures was formulated, which

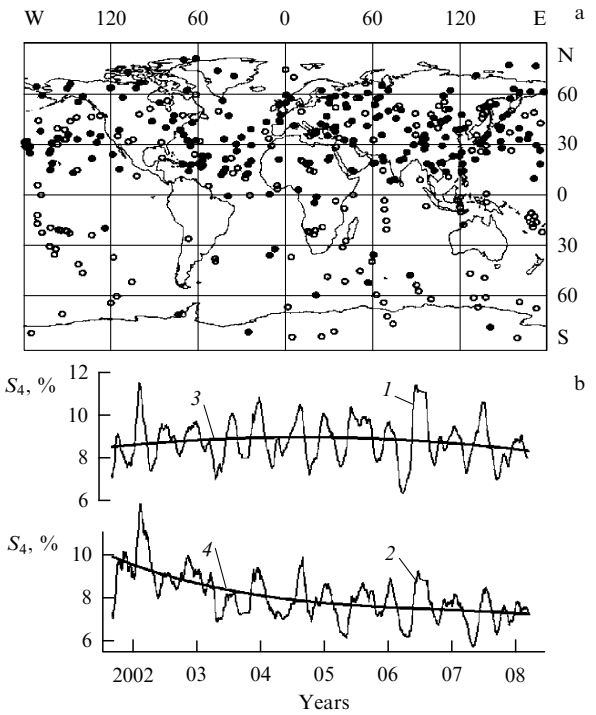

Figure 6. (a) The global distribution of intensive sporadic layers E_s according to FORMOSAT-3 satellites with the factor $S_4 > 0.12$, on June 1, 11, and 12, 2006. Black dots correspond to daytime events, circles to night-time events. (b) Time dependence of the average coefficient S_4 in the period from 2001 to 2008 according to the CHAMP data.

allowed obtaining maps of the geographic distribution of such formations.

Figure 6a shows the distribution chart for intensive sporadic E_s layers obtained according to FORMOSAT-3 satellites during the solar activity minimum for observations on June 1, 11, and 12, 2006. The chart shows an appreciable concentration of intensive sporadic layers at mid-latitudes of Earth's northern hemisphere, where the Sun's height over the horizon is maximal in June and, accordingly, the ionosphere ionization level by UV radiation is also maximal. The night-time sporadic layers are distributed over the globe more uniformly, which points to a different mechanism of their occurrence. The analysis of materials using a large-scale database including about 500,000 radio sounding sessions and created with the aid of the CHAMP satellite during 2001 – 2008 allowed obtaining information on long-term changes in the average coefficient S_4 that characterizes the fluctuation level of sounding signals. The value of the S_4 coefficient for each radio occultation session was determined as an average for the relative variations of the signal intensity, when the height h of the beam perigee exceeded 40 km, where the ionospheric influence prevails over the atmospheric influence. On average, about 200 values of S_4 were obtained within 24 hours for various regions of the globe. The data obtained in the measurement sessions were averaged over the time interval of 27 days and grouped according to latitude zones of Earth. Figure 6b shows the analysis results fot the S_4 coefficient variations in the latitude zone (lower than 55°, lines *1* and *3*), and in the polar regions (latitude higher than 55°, lines *2* and *4*). The smooth lines *3* and *4* correspond to the experimental data approximation by the method of least squares. Variations of the S_4 coefficient correlate among themselves in different geographical zones, pointing to a common mechanism of their origin, related to the effect of solar UV radiation on ionosphere ionization. The slow trend in S_4 depends on the geographical position of the measurement region. In polar regions, S_4 gradually decreases from 10% to 7% from 2001 to 2008, whereas in other regions, its value remains almost constant ($\approx 8.8\%$). The difference in slow changes of S_4 in the specified regions is apparently related to different ionization mechanisms. In the polar regions, an ionization decrease related to a reduced intensity of the solar wind influence on the ionosphere on the descending branch of solar activity is possible. In other regions, the ionization mechanism due to UV radiation of the Sun prevaile. From an analysis of long-term changes in the scintillation coefficient for radio waves sounding the ionosphere, it follows that radio signal scintillations in the high-latitude ionosphere are more sensitive to solar activity changes. The analysis also showed that it is important to study the characteristics of the signal amplitude variations of GPS satellites for investigation of the interrelation mechanism between solar activity and processes in the ionosphere and mesosphere.

The creation, realization, and development of the radio occultation monitoring method for Earth's ionosphere is described in our parers [25 – 33].

5. Conclusion

Simultaneously with foreign researchers, we suggested, realized, developed, and are improving the radio sounding method for studying plasma media of space origin: circumsolar and interplanetary plasma, the ionospheres of Mars, Venus, and Earth, and plasma shells of the Moon and comets. The difficult path of this research is partially described in Refs [1 – 33]. This problem could not be fully solved until the corresponding space-borne and ground-based means were created: long-lived spacecraft equipped with powerful, highly stable sources of radio sounding of space media, high-sensitivity systems of receiving and recording sounding signals, and high-speed information processing systems. The potential for improvement in each of these areas have not been exhausted yet and, consequently, further achievements of new interesting results in the field of Solar System research by radiophysical methods should be expected.

Advances in the development of space radiophysics at the Institute of Radioengineering and Electronics (now named after V A Kotelnikov) are linked to active support from Academician V A Kotelnikov and Professor M A Kolosov, and from numerous experts of industrial organizations that provided spacecraft launches into orbits, and the recording of signals emitted by them at deep-space communication centers.

References

1. Yakovlev O I *Kosmicheskaya Radiofizika* (Space Radiophysics) (Moscow: RFFI, 1998)
2. Yakovlev O I et al. *Astron. Zh.* **57** 790 (1980) [*Sov. Astron.* **24** 454 (1980)]
3. Efimov A I et al. *Radiotech. Elektron.* **26** 311 (1981)
4. Kolosov M A et al. *Radio Sci.* **17** 664 (1982)
5. Rubtsov S N, Yakovlev O I, Efimov A I *Kosmich. Issled.* **25** 620 (1987)
6. Yakovlev O I, Efimov A I, Rubtsov S N *Astron. Zh.* **65** 1290 (1988) [*Sov. Astron.* **32** 672 (1988)]
7. Yakovlev O I, Shishkov V I, Chashei I V *Pis'ma Astron. Zh.* **16** 163 (1990) [*Sov. Astron. Lett.* **16** 70 (1990)]

8. Efimov A I et al. *Astron. Zh.* **70** 1075 (1993) [*Astron. Rep.* **37** 542 (1993)]
9. Efimov A I et al. *Adv. Space Res.* **14** 93 (1994)
10. Efimov A I et al. *Pis'ma Astron. Zh.* **26** 630 (2000) [*Astron. Lett.* **26** 544 (2000)]
11. Efimov A I et al. *Radiotekh. Elektron.* **54** 773 (2009) [*J. Commun. Technol. Electron.* **54** 733 (2009)]
12. Efimov A I et al. *Astron. Zh.* **79** 640 (2002) [*Astron. Rep.* **46** 579 (2002)]
13. Kolosov M A et al. *Radiotech. Elektron.* **18** 2009 (1973)
14. Alexandrov Yu N et al. *Kosmich. Issled.* **14** 824 (1976)
15. Vasil'ev M B et al. *Dokl. Akad. Nauk SSSR* **218** 1298 (1974) [*Sov. Phys. Dokl.* **19** 629 (1975)]
16. Savich N A et al. *Radiotech. Elektron.* **31** 433 (1986)
17. Savich N A et al. *Radiotech. Elektron.* **31** 2113 (1986)
18. Gavrik A L, Gavrik Yu A, Samaznaev L N *Radiotekh. Elektron.* **53** 1104 (2008) [*J. Commun. Technol. Electron.* **53** 1044 (2008)]
19. Vasil'ev M B et al. *Dokl. Akad. Nauk SSSR* **212** 67 (1973) [*Sov. Phys. Dokl.* **18** 566 (1974)]
20. Savich N A et al. *Pis'ma Astron. Zh.* **12** 675 (1986) [*Sov. Astron. Lett.* **12** 283 (1986)]
21. Andreev V E, Gavrilik A L *Pis'ma Astron. Zh.* **19** 1081 (1993) [*Astron. Lett.* **19** 437 (1993)]
22. Andrianov V A, Smirnov V M *Radiotech. Elektron.* **38** 1326 (1993)
23. Smirnov V M *Radiotekh. Electron.* **46** 47 (2001) [*J. Commun. Technol. Electron.* **46** 41 (2001)]
24. Smirnov V M et al. *Radiotekh. Electron.* **53** 1112 (2008) [*J. Commun. Technol. Electron.* **53** 1052 (2008)]
25. Kucheryavenkov A I, Yakovlev O I, Kucheryavenkova I L, Samaznaev L N *Radiotekh. Electron.* **43** 945 (1998) [*J. Commun. Technol. Electron.* **43** 880 (1998)]
26. Pavelyev A et al. *Radio Sci.* **37** 1043 (2002)
27. Pavelyev A G et al. *J. Geophys. Res.* **112** A06326 (2007)
28. Pavelyev A G, Wickert J, Lion Y *Izv. Vyssh. Uchebn. Zaved. Radiofiz.* **51** 1 (2008) [*Radiophys. Quantum Electron.* **51** 1 (2008)]
29. Pavelyev A G et al. *Geophys. Res. Lett.* **36** L21807 (2009)
30. Pavelyev A G, Matyugov S S, Yakovlev O I *Radiotekh. Elektron.* **53** 1081 (2008) [*J. Commun. Technol. Electron.* **53** 1021 (2008)]
31. Yakovlev A G, Matyugov S S, Anufriev V A *Izv. Vyssh. Uchebn. Zaved. Radiofiz.* **52** 181 (2009) [*Radiophys. Quantum Electron.* **52** 165 (2009)]
32. Yakovlev O I, Wickert J, Anufriev V A *Dokl. Ross. Akad. Nauk* **427** 624 (2009) [*Dokl. Phys.* **54** 363 (2009)]
33. Yakovlev O I et al. *Acta Astronaut.* **63** 1350 (2008)

PACS numbers: 41.20.Jb, **94.20.–y**, **94.80.+g**
DOI: 10.3367/UFNe.0180.201005k.0548

Satellite radio probing and radio tomography of the ionosphere

V E Kunitsyn, E D Tereshchenko, E S Andreeva, I A Nesterov

1. Introduction

Investigations of ionospheric spatial plasma distributions are necessary in order to study the ionosphere and the physics of its processes. The ionosphere, as a medium for radio wave propagation, essentially influences the operation of various navigation, positioning, and communication systems. Therefore, investigations of the ionosphere structure are of interest for many geophysical and radiophysical applications. The existing radars and ionosondes allow only local diagnostics of the ionosphere. The creation of a sufficiently dense network of traditional means of ionospheric sounding is quite difficult and expensive. Low-orbit (like the Russian Cicada and the American Transit systems) and high-orbit (GPS/GLONASS) satellite navigation systems and the network of receivers on Earth's surface allow conducting ionosphere sounding in various directions and using tomographic methods, i.e., allow revealing the spatial structure of the ionospheric electron concentration. Currently, satellite radio tomography (RT) methods for the ionosphere are being successfully developed [1–7]. Since the early 1990s, RT systems have been operating on the basis of low-orbit (LO) navigation systems. Recently, there have been active RT studies based on the data of high-orbit (HO) navigation systems [6, 7]. To identify the different RT types, the terms 'Low-Orbit RT' and 'High-Orbit RT' are used here (LORT and HORT).

2. Low-orbit radio tomography of the ionosphere

Low-orbit navigation systems, having an almost circular orbit at the height about 1000–1150 km, and ground-based receiver chains give the opportunity to obtain series of RT data over various rays. In RT experiments, the reception of two coherent satellite signals at frequencies 150 and 400 MHz and recording of the phase difference between them (the reduced phase) is carried out on a network of several ground-based receiving stations located along a trajectory of satellites at distances of a few hundred kilometers. Measurements of the reduced phase φ at the receiving points are the data for the RT reconstruction. Integrals of the electron concentration N over the rays between a ground-based receiver and a satellite transmitter are proportional to the absolute (total) phase Φ [1, 2] that includes the unknown initial phase φ_0,

$$\alpha\lambda r_{\mathrm{e}} \int N \,\mathrm{d}\sigma = \Phi = \varphi_0 + \varphi\,, \tag{1}$$

where λ is the sounding wave length, $\mathrm{d}\sigma$ is the ray length element, r_{e} is the classical electron radius, and the proportionality coefficient α (of the order of unity) is determined by the selection of sounding frequencies.

We rewrite Eqn (1) in the operational form [4], taking a typical noncorrelated experimental noise ξ into account:

$$PN = \Phi + \xi\,. \tag{2}$$

Here, P is the projection operator transforming the two-dimensional distribution N into a set of one-dimensional projections Φ. The problem of tomographic reconstruction thus amounts to finding a solution of the set of linear integral equations (2) and finding the electron concentration N. One of the possible variants is discretization (approximation) of the projection operator P. We then obtain a corresponding set of linear equations with a discrete operator L:

$$LN = \Phi + \xi + E\,, \qquad E = LN - PN\,, \tag{3}$$

where E is the approximation error depending on the solution N. We note that Eqns (2) and (3) are equivalent if the approximation error is known. But in the data reconstruction of a real RT experiment, E is unknown and another

V E Kunitsyn, E S Andreeva, I A Nesterov Lomonosov Moscow State University, Physics Faculty, Moscow, Russian Federation
E-mail: kunitsyn@phys.msu.ru
E D Tereschenko Polar Geophysical Institute, Kola Scientific Center, Russian Academy of Sciences, Murmansk, Russian Federation

Uspekhi Fizicheskikh Nauk **180** (5) 548–553 (2010)
DOI: 10.3367/UFNr.0180.201005k.0548
Translated by S V Vladimirov; edited by A M Semikhatov